Title

Increases in brain white matter abnormalities and subcortical gray matter are linked to CD4 recovery in HIV infection

Journal

Journal of NeuroVirology, 19(4)

ISSN

1355-0284

Authors

Fennema-Notestine, Christine
Ellis, Ronald J
Archibald, Sarah L
et al.

Publication Date

2013-08-01

DOI

10.1007/s13365-013-0185-7

Peer reviewed

Published in final edited form as:
J Neurovirol. 2013 August ; 19(4): 393–401. doi:10.1007/s13365-013-0185-7.

Increases in brain white matter abnormalities and subcortical gray matter are linked to CD4 recovery in HIV infection

Christine FENNEMA-NOTESTINE[1,2], **Ronald J. ELLIS**[4], **Sarah L. ARCHIBALD**[1], **Terry L. JERNIGAN**[1,2], **Scott L. LETENDRE**[3], **Randy J. NOTESTINE**[1], **Michael J. TAYLOR**[1], **Rebecca J. THEILMANN**[2], **Michelle D. JULATON**[1], **David J. CROTEAU**[4], **Tanya WOLFSON**[6], **Robert K. HEATON**[1], **Anthony C. GAMST**[5], **Donald R. FRANKLIN Jr.**[1], **David B. CLIFFORD**[7], **Ann C. COLLIER**[8], **Benjamin B. GELMAN**[10], **Christina MARRA**[8,9], **Justin C. MCARTHUR**[11], **J. Allen MCCUTCHAN**[3], **Susan MORGELLO**[12,13], **David M. SIMPSON**[13], and **Igor GRANT**[1] **for the CHARTER Group***

[1]Department of Psychiatry, University of California, San Diego, La Jolla, CA

[2]Department of Radiology, University of California, San Diego, La Jolla, CA

[3]Department of Medicine, University of California, San Diego, La Jolla, CA

[4]Department of Neurosciences, University of California, San Diego, La Jolla, CA

[5]Department of Biostatistics and Bioinformatics, University of California, San Diego, La Jolla, CA

[6]Computational and Applied Statistics Laboratory (CASL) at the San Diego Supercomputer Center (SDSC), La Jolla, CA

[7]Department of Neurology, Washington University in St. Louis, St. Louis, MO

[8]Department of Medicine, University of Washington, Seattle, WA

[9]Department of Neurology, University of Washington, Seattle, WA

[10]Department of Pathology, University of Texas Medical Branch, Galveston, TX

[11]Department of Neurology, Johns Hopkins University, Baltimore, MD

[12]Department of Neuroscience, Mount Sinai School of Medicine, NY, NY

[13]Department of Neurology, Mount Sinai School of Medicine, NY, NY

Corresponding Author: Christine Fennema-Notestine, Ph.D. 9500 Gilman Drive # 0738, University of California, San Diego, La Jolla, CA 92093-0738 USA, Phone: (858) 246-0605, Fax: (858) 246-0665, fennema@ucsd.edu.

*The CNS HIV Anti-Retroviral Therapy Effects Research (CHARTER) group is affiliated with the Johns Hopkins University, Mount Sinai School of Medicine, University of California, San Diego, University of Texas, Galveston, University of Washington, Seattle, Washington University, St. Louis and is headquartered at the University of California, San Diego and includes: Director: Igor Grant, M.D.; Co-Directors: J. Allen McCutchan, M.D., Ronald J. Ellis, M.D., Ph.D., Thomas D. Marcotte, Ph.D.; Center Manager: Donald Franklin, Jr.; Neuromedical Component: Ronald J. Ellis, M.D., Ph.D. (P.I.), J. Allen McCutchan, M.D., Terry Alexander, R.N.; Laboratory, Pharmacology and Immunology Component: Scott Letendre, M.D. (P.I.), Edmund Capparelli, Pharm.D.; Neurobehavioral Component: Robert K. Heaton, Ph.D. (P.I.), J. Hampton Atkinson, M.D., Steven Paul Woods, Psy.D., Matthew Dawson; Virology Component: David Smith, M.D. (P.I.); Imaging Component: Christine Fennema-Notestine, Ph.D. (P.I.), Terry L. Jernigan, Ph.D., Michael J. Taylor, Ph.D., Rebecca J. Theilmann, Ph.D., John Hesselink, M.D.; Data Management Unit: Anthony C. Gamst, Ph.D. (P.I.), Clint Cushman; Statistics Unit: Ian Abramson, Ph.D. (P.I.), Florin Vaida, Ph.D.; Protocol Coordinating Component: Thomas D. Marcotte, Ph.D. (P.I.); Johns Hopkins University Site: Justin McArthur (P.I.), Mary Smith; Mount Sinai School of Medicine Site: Susan Morgello, M.D. (Co-P.I.) and David Simpson, M.D. (Co-P.I.), Letty Mintz, N.P., Cheuk Tang, Ph.D., and Thomas Naidich, M.D.; University of California, San Diego Site: J. Allen McCutchan, M.D. (P.I.), Will Toperoff, N.P.; University of Washington, Seattle Site: Ann Collier, M.D. (Co-P.I.) and Christina Marra, M.D. (Co-P.I.), Kenneth Maravilla, MD, KC Stegbauer, Ph.D., Trudy Jones, M.N., A.R.N.P.; University of Texas, Galveston Site: Benjamin Gelman, M.D., Ph.D. (P.I.), Eleanor Head, R.N., B.S.N., Gregory Chaljub, M.D.; and Washington University, St. Louis Site: David Clifford, M.D. (P.I.), Muhammad Al-Lozi, M.D., Mengesha Teshome, M.D.

The authors report no conflict of interest.

Abstract

MRI alterations in the cerebral white (WM) and gray matter (GM) are common in HIV infection, even during successful combination antiretroviral therapy (CART), and their pathophysiology and clinical significance are unclear. We evaluated the association of these alterations with recovery of CD4+ T-cells. Seventy-five HIV-infected (HIV+) volunteers in the CNS HIV Anti-Retroviral Therapy Effects Research (CHARTER) study underwent brain MRI at two visits. Multi-channel morphometry yielded volumes of total cerebral WM, abnormal WM, cortical and subcortical GM, and ventricular and sulcal CSF. Multivariable linear regressions were used to predict volumetric changes with change in current CD4 and detectable HIV RNA. On average, the cohort (79% initially on CART) demonstrated loss of total cerebral WM alongside increases in abnormal WM and ventricular volumes. A greater extent of CD4 recovery was associated with increases in abnormal WM and subcortical GM volumes. Virologic suppression was associated with increased subcortical GM volume, independent of CD4 recovery. These findings suggest a possible link between brain alterations and immune recovery, distinct from the influence of virologic suppression. The association of increasing abnormal WM and subcortical GM volumes with CD4+ T-cell recovery suggests that neuroinflammation may be one mechanism in CNS pathogenesis.

Keywords

Antiretroviral therapy; brain; CD4+ T-cell; immune recovery/reconstitution; inflammation; MRI

INTRODUCTION

Recent neuroimaging studies in HIV-infected individuals demonstrate the continued presence of altered white and gray matter despite effective combination antiretroviral therapy (CART) (Becker et al. 2011a; Becker et al. 2011b; Cardenas et al. 2009; Cohen et al. 2010a; Cohen et al. 2010b; Jernigan et al. 2011), which may reflect events associated with past severe immunosuppression, active virus, immune recovery, and persistent neuroinflammation in the central nervous system (CNS) (Ellis et al. 2007; McArthur et al. 2010). White matter pathology is reflected in both volume loss and increased abnormalities (e.g., T2 hyperintensities) on structural magnetic resonance imaging (MRI) in HIV infection (Cardenas et al. 2009; Cohen et al. 2010b; Jernigan et al. 2011). Less white matter volume has been associated with greater past immune suppression (lower nadir CD4+ T-cells) (Cohen et al. 2010b; Jernigan et al. 2011) and detectable HIV RNA in the cerebrospinal fluid (CSF) (Jernigan et al. 2011). The association between current immune status (CD4+ T-cells) and brain integrity, on the other hand, may be more complex, with higher CD4+ T-cell counts related to smaller white matter volumes in one cross-sectional study (Jernigan et al. 2011) and complex interactions in association with gray matter volumes (Cohen et al. 2010b). Subcortical gray matter atrophy also has been reported, particularly within the basal ganglia (e.g. Jernigan et al. 2005; Stout et al. 1998) where pathological studies demonstrate high viral load in the caudate nucleus (Anthony et al. 2005; Kumar et al. 2007). The pathophysiology and clinical significance of these white matter and subcortical gray matter abnormalities remain unclear in the current era of CART.

One potential source of neuroimaging alterations in CART-treated HIV-infected (HIV+) individuals is inflammation arising from the recovering immune system. Infrequently, a severe immune reconstitution inflammatory syndrome (IRIS) affects the CNS and is associated with abnormal white matter signal on MRI as well as other alterations, most often in the setting of a secondary opportunistic infection (Johnson and Nath 2010; Murdoch et al. 2007; Sidhu and McCutchan 2010). But it is unclear whether CNS IRIS represents a unique, idiosyncratic phenomenon that occurs very early in recovery or reflects an extreme inflammatory response on a continuous spectrum of CNS alterations that can occur with

immune recovery. MRI measures of abnormal white matter, and T2 hyperintensities in general, may reflect a variety of underlying pathologic processes, including inflammation and gliosis (Awad et al. 1986a; Awad et al. 1986b; Awad et al. 1987; DeCarli et al. 2005; Fazekas et al. 1993; Jernigan et al. 2011; Spilt et al. 2006; Wen et al. 2009). Similar pathological abnormalities have been reported within subcortical regions, particularly in the caudate nucleus and putamen which are known to contain more white matter and vasculature relative to neocortical gray matter (e.g. Berger et al. 2000; Meltzer et al. 1998). Neuropathological evidence exists for inflammatory processes in the basal ganglia even with successful CART treatment in HIV+ individuals (Anthony et al. 2005; Kumar et al. 2007). In fact, recent neuroimaging studies in the current CART era have noted less robust differences in subcortical volumes between HIV+ individuals and seronegative controls, despite continued associations between subcortical volumes and plasma HIV RNA (Cardenas et al. 2009; Cohen et al. 2010b). One study reported larger rather than smaller putamen volumes in HIV+ individuals, and these larger volumes were associated with higher CD4+ T-cell counts (Castelo et al. 2007). Together these findings suggest that variability in immune response and viral suppression may impact brain integrity in a dynamic manner.

We hypothesized that CD4+ T-cell recovery (increasing cell counts over time) would be associated with neuroimaging alterations that may reflect inflammation, including more white matter abnormalities and increased measured volumes of subcortical structures. Very few studies exist on quantitative measures of abnormal white matter in HIV+ individuals (Jernigan et al. 2011), particularly with respect to longitudinal change. While currently available techniques do not reliably and quantitatively measure abnormalities within gray matter, an increase in such abnormalities within the subcortical gray matter may result in a measured increase in volume (as in (Castelo et al. 2007)); such subcortical gray matter hypertrophy also has been reported in studies of stimulant users presumably related to inflammation (Jacobsen et al. 2001; Jernigan et al. 2005). We evaluated this hypothesis in a cohort of prospectively studied HIV+ individuals, most CART-treated, with serial MRI and clinical evaluations.

METHODS

Study Cohort

Participants included 75 HIV+ volunteers from the CNS HIV Anti-Retroviral Therapy Effects Research (CHARTER) study, a multicenter, prospective cohort (Table 1). Participants represented a subset of those previously described in our cross-sectional study (Jernigan et al. 2011) that each had at least one adequate follow-up MRI approximately one year later (median time to follow-up was 1.03 years [IQR 1.00,1.08]). Data were included only if there was no significant change in pulse sequence or scanner hardware or software between visits for each participant. Exclusion criteria included active opportunistic disease or severe psychiatric conditions that might preclude adequate completion of the study assessments. Five sites participated in subject recruitment and scanning: Johns Hopkins University (Baltimore, MD, n=21); Mt. Sinai School of Medicine (New York, NY, n= 14); University of California at San Diego (San Diego, CA, n= 12); University of Texas Medical Branch (Galveston, TX, n= 21); and University of Washington (Seattle, WA, n= 7). All procedures were approved by the Human Subjects Protection Committees of each participating institution and written informed consent was obtained from all study participants.

Neuromedical Assessments

Medical history was gathered, structured medical and neurological examinations were performed, and blood, urine, and cerebrospinal fluid (CSF; for those who consented to lumbar puncture) samples were collected at initial and follow-up visits. The following clinical parameters were evaluated using structured interviews and laboratory assessments as appropriate: prescription of CART, detectable plasma HIV RNA (viral load), CD4 nadir, current CD4+ T-cell count, and serologic evidence of hepatitis C virus (HCV) infection, a common comorbidity that can affect the CNS (Fletcher and McKeating 2012). Plasma and CSF viral loads were quantified by RT-PCR ultrasensitive assay (nominal lower quantitation limit 50 copies/μL). Nadir CD4+ T-cell count was based on a combination of self-report and medical records. Current CD4+ T-cell counts were measured by flow cytometry.

Multi-Channel Structural MRI protocol

All imaging was performed on General Electric 1.5T scanners that were assessed for quality annually. Four series were acquired for morphometric analysis: Series 1 and 2 were coronal acquisitions with section thickness=2.0 mm, FOV 24 cm, matrix size 256×256: 2D T2-weighted fast spin echo (FSE) with TR=5700ms, TE=90ms, ETL=16; and 2D proton density (PD) weighted FSE with TR=3700ms, TE=17ms, ETL=4. Series 3 and 4 were sagittal acquisitions with section thickness=1.3mm, FOV 24 cm, matrix size 256×256×124: 3D T1-weighted SPGR with TR=20ms, TE=6ms, flip angle=30; and 3D PD-weighted SPGR sequence with TR=20ms, TE=6ms, flip angle=5.

Because scanner differences (e.g., hardware, software, head coil upgrades) influence neuroimaging metrics (Fennema-Notestine et al. 2007; Jernigan et al. 2011), CHARTER has tracked changes in scanner configuration over time. In the present study, we have included only cases that did not experience a significant change in scanner configuration between visits, and we include a “scanner” variable in statistical analyses (see Statistical Analysis) to account for scanner-related effects between sites (Fennema-Notestine et al. 2007; Jernigan et al. 2011). Importantly, periodic site visits by UCSD staff include MR technician training and the acquisition of human phantom scans, to keep acquisition standards similar across sites.

CHARTER Morphometry

As described in Jernigan et al. (Jernigan et al. 2011), we used the multi-channel dataset in a semi-automated workflow optimized to detect subtle changes over time. Primary measures (volumes) include total cerebral white matter and abnormal white matter (e.g., hyperintense regions on T2-weighted images); subcortical (including caudate nucleus, putamen, nucleus accumbens, thalamus, and hypothalamic areas) and cerebral cortical gray matter; ventricular and sulcal CSF; and supratentorial cranial vault to account for individual differences in head size (Fig. 1) (Jernigan et al. 2011). The workflow includes image inspection for motion and other artifacts; re-slicing to a standard space; intra-subject mutual information (MI) registration (Maes 1997); bias-correction with nonparametric non-uniformity normalization (N3) (Sled et al. 1998); removal of non-brain tissue; three-tissue segmentation (gray matter, white matter and CSF); abnormal white matter designation; and anatomical labeling performed by trained anatomists. This approach includes the identification of regions of white matter with abnormal MR signal characteristics; these regions segmented as gray matter, but are anatomically located within the white matter.

For the longitudinal image processing in the present study, we employed an amplitude-based scaling factor, which accounts for any scale variations in image intensities across visits. To make the scaling robust, since localized regions may exhibit anatomical changes between scans, the scaling parameters were calculated from the difference of the means of the log transformed (skull-stripped) brain volumes. The follow-up segmentation then was

performed with the regression parameters from the first visit, after scaling of image intensities as described above for each sequence individually. Finally, the anatomical labeling for the follow-up visit was created with an algorithm that used tissue segmentations from each visit, anatomical labeling from the first visit, a set of anatomical rules, and an iterative neighborhood voting scheme. The resultant anatomically labeled output dataset reflected underlying tissue changes between visits. The algorithm allows anatomical boundaries to shift between visits due to atrophy, inflammation, or other degenerative and regenerative processes. This preliminary labeling is then reviewed and may be edited by a trained neuroanatomist, within the confines of standard rules.

Statistical Analysis

Demographic and clinical characteristics of the cohort were summarized, including an assessment of treatment status and change in CD4+ T-cell or virologic suppression. The primary analyses were designed to estimate the degree of association between CD4+ T-cell changes and longitudinal change in MRI indices of brain structural integrity, including volumetric measures of subcortical and cortical gray matter; total and abnormal white matter; and ventricular and sulcal (subarachnoid) CSF. All volumetric measures were log-transformed and CD4+ T-cell count variables were square root transformed to symmetrize the distributions and stabilize the variances. Change in MRI volumes was calculated as the difference between log-transformed volumes (Time 2 – Time 1). An initial comparison was performed simply to examine whether change in volumes was detected across time within this HIV+ cohort, regardless of factors associated with change, using a paired t-test comparing volume at Time 1 to volume at Time 2.

To address the main study question for each MRI measure, a series of multivariable linear regression models was used. In every regression model, eight covariates were included to account for variance in MRI measures that were not of primary interest in the present study (as in Jernigan et al. 2011). These control variables included: age, gender, race/ethnicity, education, time between scans, and scanner. In addition, we controlled for two common neuromedical factors known to influence brain structural integrity (Jernigan et al. 2011), serologic evidence of HCV and prior history of most severe immunosuppression (nadir CD4+ T-cell count), to focus on the effects of the more subtle changes in immune status over time.

Each model was developed to predict change in each MRI measure using a metric of change in measured current CD4+ T-cell count across visits. Change in current CD4 was assessed both as a continuous variable, calculated as the difference in square root transformed CD4 count between the two visits, and as a categorical one. The categorical approach used a change cutoff of at least +/− 50 cells/μL, reflecting numerous published reports showing this degree of CD4 change to be associated with important clinical events (Binquet et al. 2001; Moore et al. 2009; Palella et al. 2003). Categories of CD4 change included: Increasing, Decreasing, and Minimal change (less than 50 cells) groups which are characterized in Table 2. Importantly, this regression approach simultaneously examines the independent contribution of changing immune status (CD4 counts) to the change in structural volumes, while controlling for other influences. For example, a significant association between increasing current CD4 and increasing abnormal white matter volume would be the independent contribution of changing immune status, accounting for other influences on abnormal white matter volume such as age, scanner, and nadir CD4. Statistical regression results reported are the t and p values of the parameter estimate specifically associated with the relevant measure of change in current CD4 in predicting volumetric change.

In the final model, we added a variable associated with any change in detectable viral load over this same period, to assess the additional influence of virologic control. That is,

regardless of current CD4+ T-cell counts, we categorized individuals by whether viral load was detectable (nominal lower quantitation limit 50 copies/μL) over time using four categories: remained undetectable (UND-UND), changed from undetectable to detectable (UND-DET), changed from detectable to undetectable (DET-UND), and remained detectable (DET-DET) viral load levels (Table 3). The same regression approach then provides the independent contributions of immune status (Current CD4 change) and virologic control (change in detectability of viral load); for the latter, each condition was compared relative to the UND-UND group. We examined plasma HIV RNA for the full cohort and, for a subset of individuals with CSF samples (n=68), we performed the same analysis with detectable CSF HIV RNA over this same period (Table 3).

RESULTS

Subjects were mostly men (83%) with a mean age of 45.2 years (Table 1). At the initial visit, 79% (n=59) took CART and among those on CART, 69% (n=41) had achieved virologic suppression in plasma and 83% (n=49) in CSF; the median duration of the current CART regimen at Time 1 was 11 months [IQR 3, 22]. Over the follow-up period, most subjects (75%; n=56) remained consistently on CART and 5% (n=4) initiated CART, while 16% (n=12) remained off CART and 4% (n=3) switched off CART. Subjects who maintained or attained virologic suppression on CART at the second visit (n=39) had greater CD4 recovery over the follow-up interval (median change [IQR] = +35 [−37,+98]) than those not taking CART (n=15; −50 [−126,+18]) or those who failed to achieve virologic suppression on CART (n=21; −8 [−172,+103]; Kruskal-Wallis p=.03).

Over this period of time, the total HIV+ cohort demonstrated significant average loss of total cerebral white matter (t=−5.1, p<.0001) alongside average increases in ventricular (t=+3.1, p<.003) and abnormal white matter (t=+5.0, p<.0001) volumes. There was no significant change in cerebral gray matter (t=+1.1) or sulcal CSF (t=+1.7) volumes, although subcortical gray matter volume tended to increase (t=+2.0, p=.05). Since we cannot directly link these volumetric changes in our HIV+ cohort to HIV-specific factors based on this comparison alone, we report the subsequent multivariable regression models to examine the impact of immune recovery on brain structure in the context of control covariates.

After adjusting for covariates in a multivariable linear regression model, changes in CD4 cell count between the Time 1 and Time 2, considered as a continuous variable, were significantly and positively associated with changes in both abnormal white matter (*parameter estimate* t=+2.3, p=.02) and subcortical gray matter (t=+2.3, p=.03) volumes, but not with change in the other four volumetric measures. We further subdivided the cohort by extent of CD4+ T-cell count change over time, using a change cutoff of at least +/− 50 cells/μL (Binquet et al. 2001; Moore et al. 2009; Palella et al. 2003); the three categorical CD4 change groups are characterized in Table 2. The categorical CD4 change analysis confirmed the findings: there was a significant overall effect for abnormal white matter and subcortical gray matter volumes in the full regression models. The Increasing CD4 group demonstrated greater increases in abnormal white matter (t=+2.9, p=.006) and subcortical gray matter (t=+2.8, p=.008) volumes relative to the Minimal CD4 group (Figure 2). The Decreasing CD4 group had significantly greater decreases in subcortical gray matter volumes (t=−2.2, p=.03) relative to the Minimal CD4 group. There were no significant group differences in total white matter or other measured volumes.

In the final model, inclusion of detectable plasma viral load categories did not change the results of our primary analyses; that is, the Increasing CD4 group remained significantly associated with increasing abnormal white matter (t=3.1, p=.003) and increasing subcortical gray (t=2.2, p=.03) volumes. In the Decreasing CD4 group, however, subcortical gray matter

volume was no longer significantly decreasing (t=−1.44, p=.16). The distribution of viral load categories across CD4 change groups is presented in Table 3. Abnormal white matter volume did not differ significantly among the plasma viral load categories (Figure 3). Plasma viral load change categories, however, were associated with subcortical gray matter (Figure 3) and fluid measures. For those changing from detectable to undetectable plasma viral load (DET-UND), subcortical gray matter volumes increased (t=+2.8, p=.008). In contrast, for those changing from undetectable to detectable viral load (UND-DET), CSF volumes decreased (ventricles t=−2.0, p=.05; sulcal CSF t=−2.3, p=.02); subcortical gray matter volume did not change significantly (t=−1.8, p>0.10). For the group remaining detectable over time (DET-DET), ventricular volume increased (t=+3.9, p=.0003) suggestive of greater atrophy over time. For Detectable CSF viral load categories (n=68), similar findings of increased subcortical volumes for DET-UND (t=+2.3, p=.02) and greater atrophy for DET-DET (ventricles t=+2.3, p=.03) were demonstrated.

DISCUSSION

We found that during CART, recovery of CD4+ T-cells was significantly associated with increases in abnormal white matter burden and in the volume of subcortical gray matter, even while controlling for variables such as nadir CD4. CD4+ T-cell increases of at least 50 cells/μL, a clinically meaningful degree of change (Binquet et al. 2001; Moore et al. 2009; Palella et al. 2003), were seen in about 1/3 of subjects, and these subjects had the largest increases in abnormal white matter and subcortical gray matter volumes. By contrast, change in plasma viral suppression was not independently associated with abnormal white matter volume, although those changing from detectable to undetectable levels did show an increase in subcortical gray matter volumes, independent of the change in CD4. Taken together, these findings suggest a link between regional brain alterations and immune recovery, and a separate impact of virologic suppression on the brain.

Supporting the expected association between immune recovery and CART, we found greater CD4 gains among subjects initiating a new CART regimen or maintaining stable treatment than among those not taking CART or discontinuing it between visits. The median duration of an individual's current CART regimen at the initial visit was less than one year, and over three-quarters of our subjects remained on or initiated CART over the period of study. Since previous studies have shown clinically relevant CD4 recovery for up to several years after CART initiation (Koletar et al. 2004), these CD4 increases were likely CART-induced.

The differences between immunologic and virologic changes in predicting MRI alterations here may be clinically important for two reasons. First, virologic changes are most pronounced during the first three months after CART initiation. Since most of our subjects had already been on their CART regimens for about one year, and only four initiated a new regimen between visits, viral load changes seen in this study were generally modest. Thus, some of our MRI findings may not generalize to subjects who have very recently initiated CART. Second, discordant virologic and immunologic changes on CART have been previously shown in a substantial minority of individuals (Goicoechea et al. 2006; Schechter and Tuboi 2006). For example, in one series of 404 patients initiating a new CART regimen, only 70.5% experienced favorable concordant responses, defined as an increase in CD4 count of ≥50 cells/μL and achievement of undetectable plasma HIV RNA level (Tan et al. 2008).

The pathophysiology and clinical correlates of white matter abnormalities and other MR alterations in HIV infection are incompletely understood, and the differences in recovery of white matter and subcortical gray matter may be important clinically. Previous cross-sectional studies have reported that abnormal white matter in HIV+ individuals was

associated with lower nadir CD4 (Jernigan et al. 2011), while higher current CD4+ T-cell counts have been associated with larger putamen volumes (Castelo et al. 2007) and smaller overall subcortical gray matter volumes (Jernigan et al. 2011). Longitudinal studies, such as the current report, offer the opportunity to examine these neurological abnormalities as they evolve during immune recovery and treatment, potentially yielding insights into pathogenesis. We and others have previously evaluated longitudinal MR changes in the pre-CART era (Stout et al. 1998), demonstrating gray and white matter tissue loss over time, while only a few studies have examined longitudinal change among patients on CART, emphasizing continued loss in overall white matter (Cardenas et al. 2009). The present study uniquely reports quantitative change in abnormal white matter in HIV+ individuals and suggests that subtle, possibly inflammatory changes may be evident on MRI over relatively short periods of time, particularly within white and subcortical gray matter tissues, and emphasizes the importance of measuring abnormalities within these regions.

Although CD4+ T-cell and brain MR changes were contemporaneous, causal relationships cannot be inferred from our findings. Nevertheless some consideration of potential causal mechanisms is warranted to guide future hypothesis testing and study design. Known sources of abnormal white matter include vasogenic edema, astroglial proliferation, inflammatory infiltrates, injury to axons or myelin, and microvascular ischemia (Awad et al. 1986a; Awad et al. 1986b; Awad et al. 1987; DeCarli et al. 2005; Fazekas et al. 1993; Spilt et al. 2006; Wen et al. 2009). Relevant to these potential mechanisms, we found that increasing burden of white matter abnormalities occurred in the context of general reductions in white matter volume. Since vasogenic edema (characterized by excess interstitial water), astroglial proliferation, and inflammatory cell infiltration of white matter likely would drive increased rather than decreased white matter volume, these mechanisms cannot solely explain the findings. Injury to myelin and microvascular ischemia, on the other hand, might yield tissue destruction and reduced volume. Future studies could improve our understanding of brain changes in HIV infection by investigating whether one or a combination of these mechanisms underlies the increased burden of white matter abnormalities we observed with CD4 recovery on CART. Mechanisms underlying increases in subcortical gray matter volumes might include increased tissue water content or inflammatory cell infiltration, as suggested in recent studies of methamphetamine abuse (Chang et al. 2005; Jernigan et al. 2005).

It is possible and even likely that the structural MRI changes seen in this study are transient and may resolve once CD4 recovery has plateaued. Although HIV viral suppression typically is completed during the first three months of CART initiation, immune recovery lags and may continue for years (Koletar et al. 2004). Recovery of brain abnormalities could be the anatomic manifestation associated with functional (cognitive) recovery in many patients who initiate CART which also may continue for many years (McCutchan et al. 2007). Future studies should examine neuroimaging volumes at more timepoints to better assess the evolution of change over time. Additional association studies will shed light on both the potential inflammatory underpinnings, including examination of CSF inflammatory biomarkers (e.g., MCP-1), and the functional significance of these changes, examining the impact of MR changes on neurocognitive functioning, mood, and other clinically important factors.

Acknowledgments

This work was supported by awards from the National Institutes of Health for the CNS HIV Anti-Retroviral Therapy Effects Research (CHARTER) [N01 MH2205 and HHSN271201000027C] and NIH grants R01 MH079752, NIH P30 MH0625, and R21 NS069355. The views expressed in this article are those of the authors and do not reflect the official policy or position of the United States Government. Preliminary aspects of this work were presented at the Society for Neuroscience 2010 Meeting, November 2010, San Diego, CA [Program No.

764.4], and at the Fourth International Meeting on HIV Infection and the Central Nervous System: Treating the Brain in the HAART Era, July 2011, Frascati (Rome), Italy [Poster P2].

References

Anthony IC, Ramage SN, Carnie FW, Simmonds P, Bell JE. Influence of HAART on HIV-related CNS disease and neuroinflammation. J Neuropathol Exp Neurol. 2005; 64:529–36. [PubMed: 15977645]

Awad IA, Johnson PC, Spetzler RF, Hodak JA. Incidental subcortical lesions identified on magnetic resonance imaging in the elderly. II. Postmortem pathological correlations. Stroke. 1986a; 17:1090–7. [PubMed: 3810706]

Awad IA, Spetzler RF, Hodak JA, Awad CA, Carey R. Incidental subcortical lesions identified on magnetic resonance imaging in the elderly. I. Correlation with age and cerebrovascular risk factors. Stroke. 1986b; 17:1084–9. [PubMed: 3810705]

Awad IA, Spetzler RF, Hodak JA, Awad CA, Williams F Jr, Carey R. Incidental lesions noted on magnetic resonance imaging of the brain: prevalence and clinical significance in various age groups. Neurosurgery. 1987; 20:222–7. [PubMed: 3561727]

Becker JT, Maruca V, Kingsley LA, Sanders JM, Alger JR, Barker PB, Goodkin K, Martin E, Miller EN, Ragin A, Sacktor N, Selnes O. Factors affecting brain structure in men with HIV disease in the post-HAART era. Neuroradiology. 2011a

Becker JT, Sanders J, Madsen SK, Ragin A, Kingsley L, Maruca V, Cohen B, Goodkin K, Martin E, Miller EN, Sacktor N, Alger JR, Barker PB, Saharan P, Carmichael OT, Thompson PM. Subcortical brain atrophy persists even in HAART-regulated HIV disease. Brain imaging and behavior. 2011b; 5:77–85. [PubMed: 21264551]

Berger JR, Nath A, Greenberg RN, Andersen AH, Greene RA, Bognar A, Avison MJ. Cerebrovascular changes in the basal ganglia with HIV dementia. Neurology. 2000; 54:921–6. [PubMed: 10690987]

Binquet C, Chene G, Jacqmin-Gadda H, Journot V, Saves M, Lacoste D, Dabis F. Modeling changes in CD4-positive T-lymphocyte counts after the start of highly active antiretroviral therapy and the relation with risk of opportunistic infections: the Aquitaine Cohort, 1996–1997. American journal of epidemiology. 2001; 153:386–93. [PubMed: 11207157]

Cardenas VA, Meyerhoff DJ, Studholme C, Kornak J, Rothlind J, Lampiris H, Neuhaus J, Grant RM, Chao LL, Truran D, Weiner MW. Evidence for ongoing brain injury in human immunodeficiency virus-positive patients treated with antiretroviral therapy. J Neurovirol. 2009; 15:324–33. [PubMed: 19499454]

Castelo JM, Courtney MG, Melrose RJ, Stern CE. Putamen hypertrophy in nondemented patients with human immunodeficiency virus infection and cognitive compromise. Arch Neurol. 2007; 64:1275–80. [PubMed: 17846265]

Chang L, Cloak C, Patterson K, Grob C, Miller EN, Ernst T. Enlarged striatum in abstinent methamphetamine abusers: a possible compensatory response. Biological psychiatry. 2005; 57:967–74. [PubMed: 15860336]

Cohen RA, Harezlak J, Gongvatana A, Buchthal S, Schifitto G, Clark U, Paul R, Taylor M, Thompson P, Tate D, Alger J, Brown M, Zhong J, Campbell T, Singer E, Daar E, McMahon D, Tso Y, Yiannoutsos CT, Navia B. Cerebral metabolite abnormalities in human immunodeficiency virus are associated with cortical and subcortical volumes. J Neurovirol. 2010a; 16:435–444. [PubMed: 20961212]

Cohen RA, Harezlak J, Schifitto G, Hana G, Clark U, Gongvatana A, Paul R, Taylor M, Thompson P, Alger J, Brown M, Zhong J, Campbell T, Singer E, Daar E, McMahon D, Tso Y, Yiannoutsos CT, Navia B. Effects of nadir CD4 count and duration of human immunodeficiency virus infection on brain volumes in the highly active antiretroviral therapy era. J Neurovirol. 2010b; 16:25–32. [PubMed: 20113183]

DeCarli C, Fletcher E, Ramey V, Harvey D, Jagust WJ. Anatomical mapping of white matter hyperintensities (WMH): exploring the relationships between periventricular WMH, deep WMH, and total WMH burden. Stroke. 2005; 36:50–5. [PubMed: 15576652]

Ellis R, Langford D, Masliah E. HIV and antiretroviral therapy in the brain: neuronal injury and repair. Nature reviews Neuroscience. 2007; 8:33–44.

Fazekas F, Kleinert R, Offenbacher H, Schmidt R, Kleinert G, Payer F, Radner H, Lechner H. Pathologic correlates of incidental MRI white matter signal hyperintensities. Neurology. 1993; 43:1683–9. [PubMed: 8414012]

Fennema-Notestine C, Gamst AC, Quinn BT, Pacheco J, Jernigan TL, Thal L, Buckner R, Killiany R, Blacker D, Dale AM, Fischl B, Dickerson B, Gollub RL. Feasibility of multi-site clinical structural neuroimaging studies of aging using legacy data. Neuroinformatics. 2007; 5:235–45. [PubMed: 17999200]

Fletcher NF, McKeating JA. Hepatitis C virus and the brain. Journal of viral hepatitis. 2012; 19:301–6. [PubMed: 22497808]

Goicoechea M, Smith DM, Liu L, May S, Tenorio AR, Ignacio CC, Landay A, Haubrich R. Determinants of CD4+ T cell recovery during suppressive antiretroviral therapy: association of immune activation, T cell maturation markers, and cellular HIV-1 DNA. The Journal of Infectious Diseases. 2006; 194:29–37. [PubMed: 16741879]

Jacobsen LK, Giedd JN, Gottschalk C, Kosten TR, Krystal JH. Quantitative morphology of the caudate and putamen in patients with cocaine dependence. The American Journal of Psychiatry. 2001; 158:486–9. [PubMed: 11229995]

Jernigan TL, Archibald SL, Fennema-Notestine C, Taylor MJ, Theilmann RJ, Julaton MD, Notestine RJ, Wolfson T, Letendre SL, Ellis RJ, Heaton RK, Gamst AC, Franklin DR Jr, Clifford DB, Collier AC, Gelman BB, Marra C, McArthur JC, McCutchan JA, Morgello S, Simpson DM, Grant I. Clinical factors related to brain structure in HIV: the CHARTER study. Journal of NeuroVirology. 2011; 17:248–57. [PubMed: 21544705]

Jernigan TL, Gamst AC, Archibald SL, Fennema-Notestine C, Mindt MR, Marcotte TD, Heaton RK, Ellis RJ, Grant I. Effects of methamphetamine dependence and HIV infection on cerebral morphology. The American Journal of Psychiatry. 2005; 162:1461–72. [PubMed: 16055767]

Johnson T, Nath A. Neurological complications of immune reconstitution in HIV-infected populations. Ann N Y Acad Sci. 2010; 1184:106–20. [PubMed: 20146693]

Koletar SL, Williams PL, Wu J, McCutchan JA, Cohn SE, Murphy RL, Lederman HM, Currier JS. Long-term follow-up of HIV-infected individuals who have significant increases in CD4+ cell counts during antiretroviral therapy. Clinical Infectious Diseases. 2004; 39:1500–6. [PubMed: 15546087]

Kumar AM, Borodowsky I, Fernandez B, Gonzalez L, Kumar M. Human immunodeficiency virus type 1 RNA Levels in different regions of human brain: quantification using real-time reverse transcriptase-polymerase chain reaction. J Neurovirol. 2007; 13:210–24. [PubMed: 17613711]

Maes F, Collignon A, Vandermeulen D, Marchal G, Suetens P. Multimodality image registration by maximization of mutual information. IEEE Trans on Medical Imaging. 1997; 16:187–198.

McArthur JC, Steiner J, Sacktor N, Nath A. Human immunodeficiency virus-associated neurocognitive disorders: Mind the gap. Ann Neurol. 2010; 67:699–714. [PubMed: 20517932]

McCutchan JA, Wu JW, Robertson K, Koletar SL, Ellis RJ, Cohn S, Taylor M, Woods S, Heaton R, Currier J, Williams PL. HIV suppression by HAART preserves cognitive function in advanced, immune-reconstituted AIDS patients. AIDS. 2007; 21:1109–17. [PubMed: 17502721]

Meltzer CC, Wells SW, Becher MW, Flanigan KM, Oyler GA, Lee RR. AIDS-related MR hyperintensity of the basal ganglia. AJNR Am J Neuroradiol. 1998; 19:83–9. [PubMed: 9432162]

Moore DM, Harris R, Lima V, Hogg B, May M, Yip B, Justice A, Mocroft A, Reiss P, Lampe F, Chene G, Costagliola D, Elzi L, Mugavero MJ, Monforte AD, Sabin C, Podzamczer D, Fatkenheuer G, Staszewski S, Gill J, Sterne JA. Effect of baseline CD4 cell counts on the clinical significance of short-term immunologic response to antiretroviral therapy in individuals with virologic suppression. Journal of Acquired Immune Deficiency Syndromes. 2009; 52:357–63. [PubMed: 19668084]

Murdoch DM, Venter WD, Van Rie A, Feldman C. Immune reconstitution inflammatory syndrome (IRIS): review of common infectious manifestations and treatment options. AIDS research and therapy. 2007; 4:9. [PubMed: 17488505]

Palella FJ Jr, Deloria-Knoll M, Chmiel JS, Moorman AC, Wood KC, Greenberg AE, Holmberg SD. Survival benefit of initiating antiretroviral therapy in HIV-infected persons in different CD4+ cell strata. Annals of internal medicine. 2003; 138:620–6. [PubMed: 12693883]

Schechter M, Tuboi SH. Discordant immunological and virological responses to antiretroviral therapy. The Journal of antimicrobial chemotherapy. 2006; 58:506–10. [PubMed: 16854959]

Sidhu N, McCutchan JA. Unmasking of PML by HAART: unusual clinical features and the role of IRIS. Journal of neuroimmunology. 2010; 219:100–4. [PubMed: 19962769]

Sled JG, Zijdenbos AP, Evans AC. A nonparametric method for automatic correction of intensity nonuniformity in MRI data. IEEE Trans Med Imaging. 1998; 17:87–97. [PubMed: 9617910]

Spilt A, Goekoop R, Westendorp RG, Blauw GJ, de Craen AJ, van Buchem MA. Not all age-related white matter hyperintensities are the same: a magnetization transfer imaging study. AJNR Am J Neuroradiol. 2006; 27:1964–8. [PubMed: 17032876]

Stout JC, Ellis RJ, Jernigan TL, Archibald SL, Abramson I, Wolfson T, McCutchan JA, Wallace MR, Atkinson JH, Grant I. Progressive cerebral volume loss in human immunodeficiency virus infection: a longitudinal volumetric magnetic resonance imaging study. HIV Neurobehavioral Research Center Group. Archives of Neurology. 1998; 55:161–8. [PubMed: 9482357]

Tan R, Westfall AO, Willig JH, Mugavero MJ, Saag MS, Kaslow RA, Kempf MC. Clinical outcome of HIV-infected antiretroviral-naive patients with discordant immunologic and virologic responses to highly active antiretroviral therapy. Journal of Acquired Immune Deficiency Syndromes. 2008; 47:553–8. [PubMed: 18285713]

Wen W, Sachdev PS, Li JJ, Chen X, Anstey KJ. White matter hyperintensities in the forties: their prevalence and topography in an epidemiological sample aged 44–48. Hum Brain Mapp. 2009; 30:1155–67. [PubMed: 18465744]

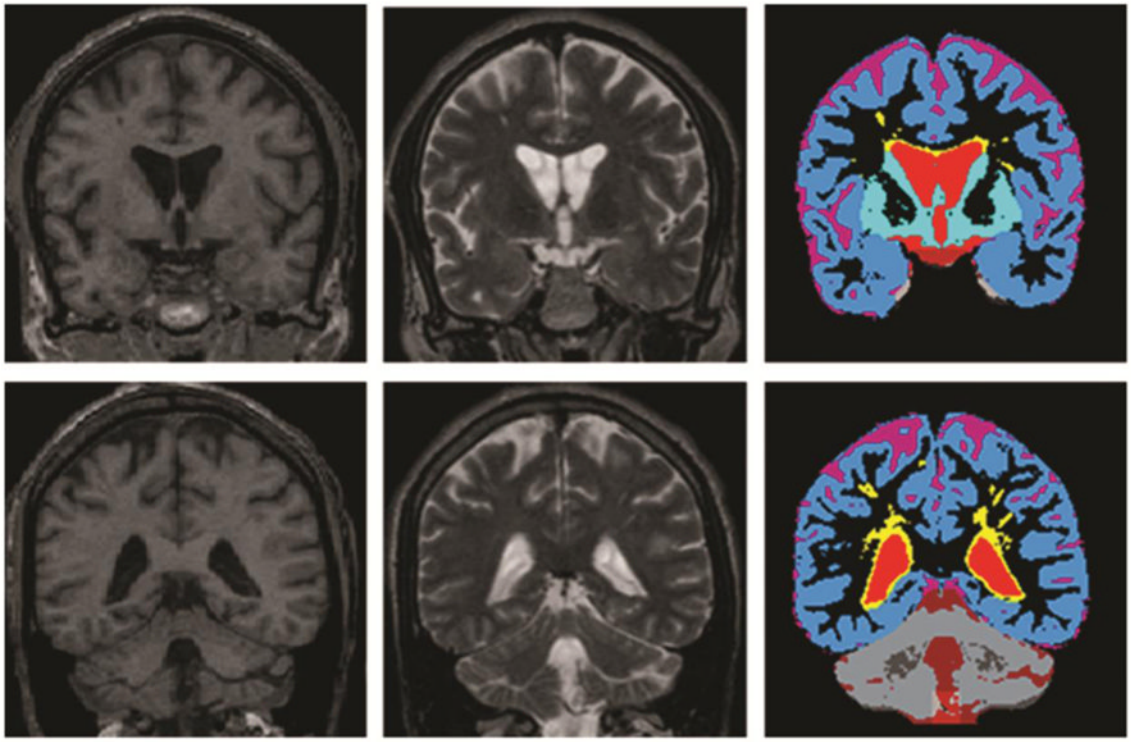

Fig. 1. CHARTER Morphometry

Example coronal sections of T1 (left), T2 (middle), and anatomical segmentation (right) for anterior (top) and posterior (bottom) sections. Volumes include: abnormal (yellow) and total (yellow+black) white matter; cortical (blue) and subcortical (cyan) gray matter; ventricular (red) and subarachnoid, or sulcal, (purple) CSF.

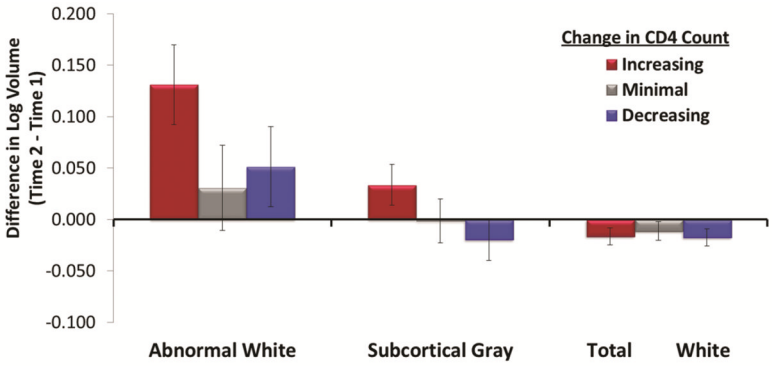

Fig. 2. Volumetric Change by CD4 Change Category

Estimated marginal means of change in log volume by CD4 Change Category, accounting for all other variables in the full regression model. Error bars = standard error.

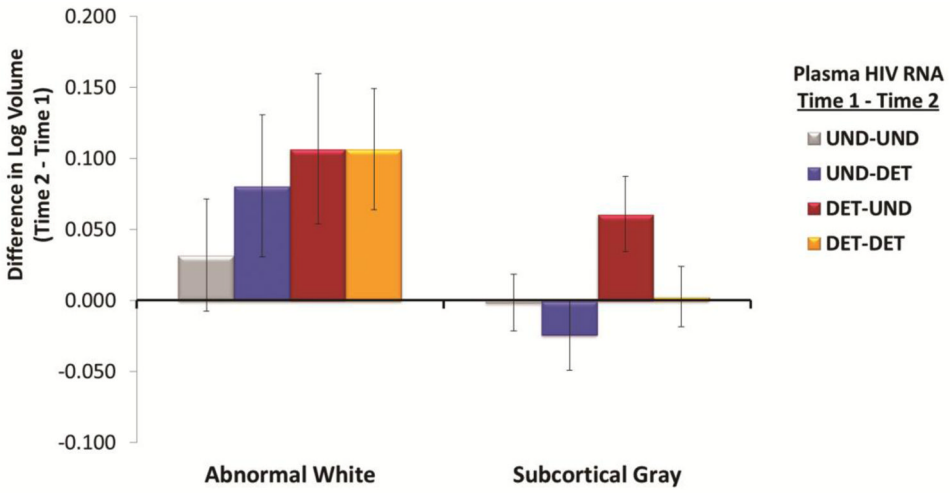

Fig. 3. Volumetric Change by Status of Detectable Plasma HIV RNA (viral load) Category

Estimated marginal means of change in log volume by Change in Plasma Viral Load Status Category, accounting for all other variables in the final full regression model including Change in CD4 Category. UND=undetectable plasma viral load; DET=detectable plasma viral load. Error bars = standard error.

Table 1
Demographic and Clinical Characteristics

Values reported include mean (sd); percent (%) of the cohort with given characteristics; and median [IQR or interquartile range].

	Initial Visit	Follow-up* Visit
Age in Years	45.2 (7.8)	--
Sex (% Male)	83%	--
Ethnicity		
African American	51%	--
Caucasian	39%	--
AIDS	71%	75%
Nadir CD4 copies/μL	108 [13,212]	93 [12,208]
Current CD4 copies/μL	456 [234,606]	451 [279,645]
Duration of HIV Infection, in months	137 [85–184]	149 [96,201]
Plasma HIV RNA (VL) Detectable	44%	45%
CSF HIV RNA (VL) Detectable	33%	25%
HCV sero-positive	39%	--
On CART	79% (n=59)	80% (n=60)
Duration current CART regimen, months	11 [3,22]	14 [5,26]
PI-based	59%	63%
NNRTI-based	32%	30%
PI/NNRTI-based	3%	3%
Other regimen type	5%	3%
ART Naïve	5.3%	5.3%

Abbreviations: CART, combination antiretroviral therapy; sd, standard deviation; VL, viral load, log10 copies/μL.

*Follow-up visit occurred approximately one year after initial visit (median=1.03, IQR=[0.997,1.079]).

Table 2
Categorical CD4 Change Group Characteristics

CD4+ T-cell counts reflect the median [IQR] for each visit or change.

CD4 Change Group	*n*	Initial CD4	Follow-up CD4	Change in CD4
Increasing CD4 (≥50)	25	360 [176,518]	514 [379,672]	+163 [81,272]
Decreasing CD4 (≥50)	26	570 [364,850]	412 [171,646]	−126 [−214, −99]
Minimal CD4 change (−49 to +49)	24	413 [242,594]	412 [248,630]	+11 [−8,21]

Table 3

Detectable HIV RNA (viral load) Characteristics for Plasma and CSF by CD4 Change Group

Proportion within CD4 Change group is reported with number of cases in parentheses.

	HIV RNA (Viral load) Status Time 1 → Time 2			
	UNDetectable → UNDetectable	**UNDetectable → DETectable**	**DETectable → UNDetectable**	**DETectable → DETectable**
Change Group*	***plasma n=32 CSF n=42***	***n=10 n=4***	***n=9 n=9***	***n=24 n=13***
Increasing CD4				
Plasma	52% (13)	8% (2)	20% (5)	20% (5)
CSF	66% (15)	4% (1)	26% (6)	4% (1)
Decreasing CD4				
Plasma	27% (7)	23% (6)	4% (1)	46% (12)
CSF	52% (12)	4% (1)	4% (1)	40% (9)
Minimal CD4				
Plasma	50% (12)	8% (2)	13% (3)	29% (7)
CSF	68% (15)	9% (2)	9% (2)	14% (3)

*The Increasing CD4 change group increased by ≥50 cells/μL; the Decreasing CD4 group decreased by ≥50 cells/μL; and the Minimal CD4 change group changed <50 cells/μ.